LRP 618/98 October 1998

Stabilization of Neoclassical Tearing Modes Using a Continuous Localized Current Drive

A. Pletzer, F.W. Perkins

Stabilization of neoclassical tearing modes using a continuous localized current drive

A. Pletzer*
Centre de Recherches en Physique des Plasmas
Association Euratom – Confédération Suisse
PPB-Ecublens
CH-1015 Lausanne, Switzerland

F. W. Perkins
ITER-JCT
11035 N. Torrey Pines Rd
La Jolla, CA 92037

The stability of a test equilibrium relevant to the International Thermonuclear Experimental Reactor (ITER) has been studied within the framework of the neoclassical island evolution theory. The most unstable modes, with the most positive matching index Δ', have been found by solving numerically the marginal magnetohydrodynamic stability equation in toroidal geometry to have 3/2, 2/1 and 4/3 helicities.

Quasi-linear effects resulting from the current profile flattening as the island develops are important and stabilizing. Nonetheless, large saturated islands are predicted to arise due to a combination of strong bootstrap current drive and weakly negative Δ'.

We propose to apply a Continuous Current Drive (CCD) at the unstable rational surface to locally tailor the current profile by inducing favourable current gradients on either side of the rational surface. An important reduction of the island size, which is proportional to the current drive and inversely proportional to the square of the current channel width can then be achieved. The so obtained stabilization relies on the removal of free energy in the outer region and can thus be regarded as a Δ' effect.

I. INTRODUCTION

Tearing modes are detrimental to confinement and, in some cases, they can lead to a disruption. One driving mechanism for tearing modes when the ratio of pressure gradient to magnetic shear is negative, is the suppression of the neoclassical bootstrap current as the island grows and the pressure flattens [1,2]. Most tokamaks have now routinely observed these modes, which are associated with the observation of a pressure limit below the one predicted by ideal magnetohydrodynamics (MHD). In addition, the drive may be provided by the free-energy source [3,4] as measured by the resistive matching index Δ', which is proportional to the jump in derivative of the radial magnetic perturbation across the singular surface [5]. A value of $\Delta' < 0$ is regarded as stabilizing, though not sufficient to totally suppress an island in the presence of a destabilizing neoclassical bootstrap current drive, leading to a saturation width $\sim (-\Delta')^{-1}$.

Experimentally, neoclassical tearing modes first tend to develop at the mode rational surfaces $q = m/n$ with poloidal mode $m = 3$ and toroidal mode $n = 2$, where Δ' tends to be negative but weak. Islands with the 3/2 helicity are not, however, persistently observed and the general understanding is that the island is metastable; its width must exceed a particular threshold to grow and reach the full saturation width. This threshold can be due to inertial, diamagnetic flow, finite Larmor radius, banana width or other effects, all of which only contribute at small island width (typically $w < 1cm$). These effects are expected to be stabilizing. Two models are presently competing to explain the existence of such a threshold, one based on finite perpendicular transport [6] and the other on the polarization current due to diamagnetic drift [7]. The second theory by Wilson *et al.* appears at present to better agree with experimental results obtained in the DIII-D tokamak [8]. However, this

*Present address: Princeton Plasma Physics Research Laboratory, P. O. Box 451, Princeton, NJ 08543 (pletzea@pppl.gov)

threshold is currently predicted to decrease as the plasma becomes hotter and collisionless. Thus, a magnetic perturbation 2/2 following a sawtooth crash [9] is likely to drive a 3/2, or possibly a 4/3, mode unstable in ITER.

However, the threshold is not the only stabilizing effect coming into play. In § II we derive the quasi-linear stabilization due to the flattening of the current profile, which amounts to a $w \log w$ term [10]. This stabilization is stronger than the term proportional to the equilibrium current gradient and to w, used by other authors [11,12]. A stronger quasi-linear stabilization could explain why modes with $\Delta' > 0$ do not necessarily lead to a disruption in spite of the presence of the drive due to the bootstrap current.

Even so, the inclusion of the quasi-linear stabilizing effect in the island equation can potentially produce large saturated island of width well in excess of $> 10\%$ of the minor radius. In ITER, this is due to a combination of weak Δ' and strong bootstrap current at the 3/2 and 2/1 rational surfaces.

To further mitigate the growth of the island, it has recently been proposed to aim a modulated electron cyclotron current drive [13–15] at the O-point of the island in order to overcome the bootstrap current deficit. This scheme relies on good synchronization. We show however that robust stabilization can be achieved by applying instead a *Continuous* Current Drive (CCD) about the rational surface, by means of a simple one-dimensional model developed in § III. This model also reveals a stabilization loss when the current drive is not aimed accurately at the rational surface. The stabilization is due favourable current gradients inside and outside the rational surface. The efficiency of the CCD scheme is comparable to the modulated scheme. In § IV, we confirm the validity of the simple one-dimensional model by applying it first to a cylindrical plasma and then to an ITER equilibrium.

II. INNER LAYER

A. Magnetic topology

To describe the island evolution in thin layers about the rational surfaces, we take the plasma to be cylindrical and of periodicity $2\pi R$ along the toroidal z direction, R being the major radius. The magnetic field then reads

$$\mathbf{B} = B_z \hat{\mathbf{z}} + \hat{\mathbf{z}} \times \nabla \psi$$

with

$$\psi = \psi_0 + A \cos m\hat{\theta} \tag{1}$$

being the helical flux, which is composed of an equilibrium part

$$\psi_0 = \int^r dr' B_\theta \left(1 - \frac{q(r')}{q_s}\right) = -B_\theta \frac{q_s'}{q_s} \frac{x^2}{2} + \mathcal{O}(x^3) \quad ; \quad x \equiv r - r_s$$

and a small perturbation $A \cos m\hat{\theta}$. The small perturbation is resonant

$$\hat{\theta} \equiv \theta - \frac{1}{q_s} \frac{z}{R}$$

at the mode rational surface, where the safety factor $q(r_s) \equiv q_s = m/n$. Introducing the normalized helical flux

$$s \equiv \tfrac{1}{2}(1 - \psi/A),$$

(1) then becomes

$$s = \frac{x^2}{w^2} + \sin^2 \frac{m\hat{\theta}}{2} \tag{2}$$

where

$$w \equiv 2 \left| \frac{L_q A}{B_\theta} \right|^{1/2} \tag{3}$$

is the island *half*-width with $L_q \equiv q_s/q_s' \equiv r_s/\hat{s}$ and $\hat{s}$ being the shear $r_s q_s'/q_s$. Equation (2) yields an island topology with "trapped" ($0 < s < 1$) and "circulating" field lines ($0 < s < 1$).

B. Island evolution equation

The procedure to obtain the island evolution equation is standard [16] and will only be sketched here. One uses Ohm's law along the z direction

$$E_z + \mathbf{v}\cdot\nabla\psi = \eta\,(J - J_{neo}) \tag{4}$$

and $E_z = \partial\psi/\partial t = (\partial A/\partial t)\cos m\hat{\theta}$, where

$$J - J_{neo} = \nabla^2\psi \tag{5}$$

represents the inductive component of the perturbed current and η the resistivity along the dominant $\mathbf{B}$ direction. The convective derivative $\mathbf{v}\cdot\nabla\psi$ is annihilated after applying

$$\langle\bullet\rangle \equiv \oint_s d\hat{\theta}\left(\frac{\partial s}{\partial x}\right)^{-1} \bullet \Big/ \oint_s d\hat{\theta}\left(\frac{\partial s}{\partial x}\right)^{-1}$$

to (4). Upon writing $J = J_0 + J_0' x$, J_0 is then eliminated by adding the average of (4) to equation (5), which yields

$$\nabla^2 A\cos m\hat{\theta} = \frac{1}{\eta}\frac{\partial A}{\partial t}\left\langle\cos m\hat{\theta}\right\rangle + J_0'\left(\langle x\rangle - x\right) - \left(\langle J_{neo}\rangle - J_{neo}\right). \tag{6}$$

The bootstrap current J_{neo} is proportional to the gradient of the fluctuating pressure, which decreases rapidly from the rational surface position. In the limit of x large, we get

$$\frac{\partial^2 A}{\partial x^2}\cos m\hat{\theta} \approx \mathcal{O}(A^2) + \frac{\lambda_s}{r_s x} A\cos m\hat{\theta}, \tag{7}$$

where

$$\lambda_s = -\frac{r_s q_s J'(r_s)}{q'(r_s) B_\theta}. \tag{8}$$

The importance of the equilibrium current gradient term in (6) is readily verified by noting that (7) reproduces the regular singular point at the rational surface, which arises in the outer region equation [17,18] in the limit of infinitesimal island width. Without this singularity, there could be no asymptotic matching procedure. The current gradient has been omitted in most previous works [16,19,2,20–22,7].

C. Matching data in the low β approximation

The equation describing the temporal evolution of the island width is derived by applying $\frac{1}{\pi A}\int_{-\infty}^{\infty} dx \int_{-\pi}^{\pi} d\theta \cos m\hat{\theta}$ onto (6). Expanding

$$A = A_0 + A_\pm' x + \cdots$$

where $+$ stands for $x > 0$ and $-$ denotes $x < 0$, one finds that A_0 gives the dominant contribution (6), except for the current gradient term for which it cancels. Upon using the approximation [23]

$$x = \pm w\left(s - \sin^2\frac{m\hat{\theta}}{2}\right)^{1/2} + \frac{w^2}{4}\frac{A_\pm'}{A_0}\cos m\hat{\theta} + \cdots$$

one then gets,

$$\frac{A_+' - A_-'}{A_0} = \frac{2k\tau_R}{r_s}\frac{d}{dt}\left(\frac{w}{r_s}\right) - k\lambda_s\frac{A_+' + A_-'}{A_0}w + 2.3\sqrt{\epsilon_s}\beta_p\frac{L_q}{L_p}\left(\frac{r_s}{w}\right) \tag{9}$$

where $k \approx 0.83$, and $\tau_R \equiv r_s^2/\eta$ is the resistive time scale. The contribution from the bootstrap current was obtained using the formula given in Ref. [6], with $\epsilon_s = r_s/R$, $\beta_p = 2p/B_\theta^2$ and $L_q/L_p = -p'/q'$, all quantities being evaluated at the rational surface position.

The first term of (9) gives the well-known Δ' parameter and the last term the matching index of ballooning parity. These matching data are obtained by solving the outer region equation [24]. In the outer region, the solution has the following asymptotic behaviour [25],

$$\frac{A(x)}{A_0} = \left|\frac{x}{r_s}\right|^{\frac{1}{2}-\mu}\left(1+\frac{\lambda_s}{1-2\mu}x+\cdots\right) + \frac{\Delta'}{2}\left|\frac{x}{r_s}\right|^{\frac{1}{2}+\mu}(1+\cdots)+\frac{\Gamma'}{2}\left|\frac{x}{r_s}\right|^{\frac{1}{2}+\mu}\mathrm{sgn}x\,(1+\cdots) \tag{10}$$

as $x \to 0$. The first term in (10) represents the large solution, which is assumed here to be of even parity to leading order. The remaining two terms are the small solutions of even (odd) parity with leading coefficients $\Delta'/2$ ($\Gamma'/2$). In (10), μ is given by the equilibrium and is equal to $\sqrt{-D_I}$ where D_I is the Mercier stability index against ideal localized modes (see e.g [26]). In the $\beta \to 0$ limit we have $\mu \to \frac{1}{2}$, this is also the limit where the next order terms in the large solution (10) become singular so that, in order to get a finite solution, Γ' *must also become infinite.* Assuming for the moment $\mu - \frac{1}{2}$ to be small but not zero, we proceed and find the average of the normalized radial derivative

$$\frac{A'_+ + A'_-}{A_0} \to \tilde{\Gamma}' + 2\lambda_s \ln\left|\frac{w}{r_s}\right| + \mathcal{O}(1-2\mu) \tag{11}$$

at distance $\pm w$, where

$$\tilde{\Gamma}' \equiv \Gamma' - \frac{\lambda_s}{\mu - \frac{1}{2}}$$

is the odd-parity renormalized index [27], which is well defined when $\beta \to 0$. In (11) we used the fact that the first order term proportional to λ_s in the large solution has almost the same power as the leading term of the small solution. Alternatively, we could have taken the $\beta = 0$ limit before-hand and assume a Frobenius expansion (10) that includes the logarithmic term. Both approaches give the same result.

Substituting (11) in (9), the island width evolution equation thus becomes

$$r_s\Delta' = \frac{1.64\tau_R}{r_s}\frac{d}{dt}\left(\frac{w}{r_s}\right) - 1.64 r_s\lambda_s^2\left(\frac{w}{r_s}\right)\ln\left|\frac{w}{r_s}\right| - 0.83 r_s\lambda_s\tilde{\Gamma}'\left(\frac{w}{r_s}\right) + 2.3\sqrt{\epsilon_s}\beta_p\frac{L_q}{L_p}\left(\frac{r_s}{w}\right). \tag{12}$$

This equation describes the nonlinear evolution of the tearing-mode normalized half-width w/r_s. The first two terms yield the Rutherford equation [16] with the island growing linearly in time and Δ'. For convenience, we may absorb the contributions from ideal MHD into a matching index

$$\Delta(w) \equiv \Delta' + 1.64\lambda_s^2\left(\frac{w}{r_s}\right)\ln\left|\frac{w}{r_s}\right| + 0.83\lambda_s\tilde{\Gamma}'\left(\frac{w}{r_s}\right), \tag{13}$$

that incorporates finite-island-width effects. The index Δ' can be computed by solving the marginal stability equation in the outer, ideal region using the PEST-3 code [28]. The parameter λ_s is given by (8) and is a property of the unperturbed equilibrium at r_s. The last term is the quasi-linear stabilization obtained by White and Monticello [11], and Zakharov *et al.* [23]. However, these authors have failed to recognize the singular nature of (11), which is at the origin of the logarithmic term.

One aspect that has been overlooked is that

$$\frac{A'_+ - A'_-}{A_0} \to (1-2\mu)\frac{r_s}{w} + \Delta' + \cdots$$

also produces an additional term at distance $\pm w$. This term represents a Glasser, Greene and Johnson stabilization [26] for the island evolution equation ($\mu \approx \frac{1}{2} - D_R$ where D_R is the resistive Mercier index). A more rigorous approach [19] gives a pressure stabilization proportional to $3.1 D_R r_s/w$.

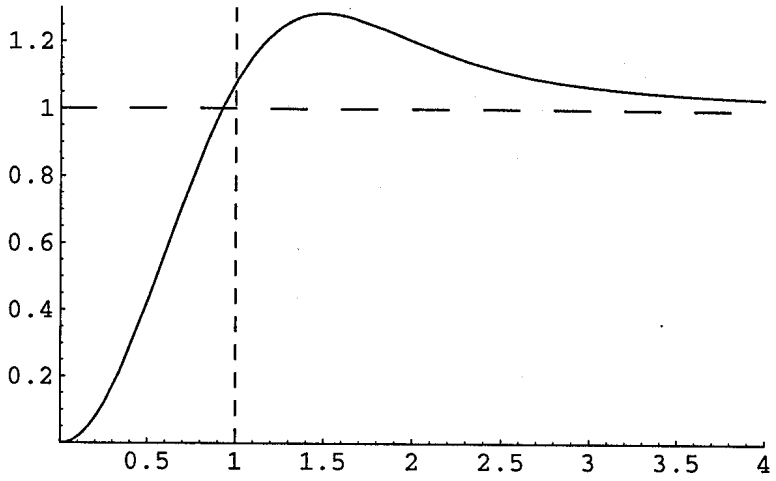

FIG. 1. Function $h(\alpha)$ representing the stabilization/destabilization factor. The Gaussian current density is stabilizing for $h(\alpha) < 1$ but destabilizing for $h(\alpha) > 1$.

III. LOCALIZED GAUSSIAN CURRENT AT THE RATIONAL SURFACE

Tearing modes can be made more stable by tailoring [29] the current profile in the vicinity of rational surfaces. This is best seen by inspection of the ideal, marginal stability equation

$$\frac{1}{r}\frac{d}{dr}r\frac{d\Psi}{dr} - \frac{\lambda(r)}{r(r-r_s)}\Psi - \frac{m^2}{r^2}\Psi = 0, \tag{14}$$

for the radial magnetic field perturbation Ψ in the large aspect ratio limit. Equation (14) has the same structure as (7) with Ψ and A having the same singular behaviour as $x \to 0$. Here, the function

$$\lambda(x) \equiv \frac{Rq_s J'(x)(x-1)}{B_z[q_s/q(x)-1]} \tag{15}$$

is well-behaved and proportional to the current gradient $J'(r)$, which captures all the equilibrium features and provides the source of instability. Note that in the limit of $x \to 0$ we recover (8). In the absence of the λ term, the solutions to (14) are $r^{\pm m}$. Requiring Ψ to be regular at the $r = 0$ magnetic axis and assuming a conducting wall at infinity, we obtain for the matching index

$$r_s\Delta' \equiv \frac{1}{\Psi(r_s)}\left(\left.\frac{d\Psi}{dr}\right|_{r_s+} - \left.\frac{d\Psi}{dr}\right|_{r_s-}\right) = -2m, \tag{16}$$

which is negative and thus stable [30]. The destabilizing effect of $\lambda > 0$ for $r < r_s$ is most apparent when using Furth *et al.*'s [3] expression

$$r_s\Delta' = -\frac{1}{\Psi(r_s)^2}\int_0^a dr r\left\{\left(\frac{d\Psi}{dr}\right)^2 + \left(\frac{\lambda}{r-r_s} + \frac{m^2}{r}\right)\Psi^2\right\}, \tag{17}$$

which is obtained after multiplying (14) by Ψ and taking the principal part of the integral across the plasma. Clearly, if the current gradient is made positive where $r < r_s$ and negative in the region where $r > r_s$, this can only be favourable to stability (i.e. Δ' decreases).

For the specific case of a Gaussian current density profile,

$$J(x) = J_{CD} \exp\left[-\left(\frac{x}{\sigma} - \alpha\right)^2\right] \tag{18}$$

of radial extent σ, which peaks at $x = \alpha\sigma$ (x being the distance from the rational surface), (14) can be written approximately as

$$\Psi''(x) \approx \frac{4}{\hat{s}\sigma}\left(\frac{J_{CD}}{J_q}\right)\frac{(x/\sigma - \alpha)\exp\left[-(x/\sigma - \alpha)^2\right]}{x}, \tag{19}$$

where $J_q \equiv 2B_z/Rq_s$, and after normalizing Ψ to one at r_s. Assuming the constant Ψ approximation to hold, (19) can be integrated analytically, yielding

$$\Delta' \approx -\frac{4\sqrt{\pi}}{\hat{s}\sigma}\left(\frac{J_{CD}}{J_q}\right)[1 - h(\alpha)], \tag{20}$$

where

$$h(\alpha) = \frac{\alpha}{\sqrt{\pi}}\wp\int_{-\infty}^{\infty} dx \frac{\exp\left[-(x/\sigma - \alpha)^2\right]}{x} = -i\,\alpha\sqrt{\pi}\mathrm{erf}(i\alpha)\,\exp\left(-\alpha^2\right) \tag{21}$$

whose behaviour is shown in Fig. 1 and, which can be expressed in term of the error function. According to this model, the best results are achieved by aiming at the rational surface position ($\alpha = 0$) and taking a narrow channel width (σ small). The stabilization degrades, however, as $|\alpha|$ increases; when $|\alpha| > 0.9$, Δ' becomes positive and reaches a maximum at $\alpha \approx 1.6$. At this point, the Gaussian bump sits on either side of the rational surface and the stabilizing effect is lost. Thus, the rule of thumb to get a stabilizing effect is

$$|\alpha| < 0.9. \tag{22}$$

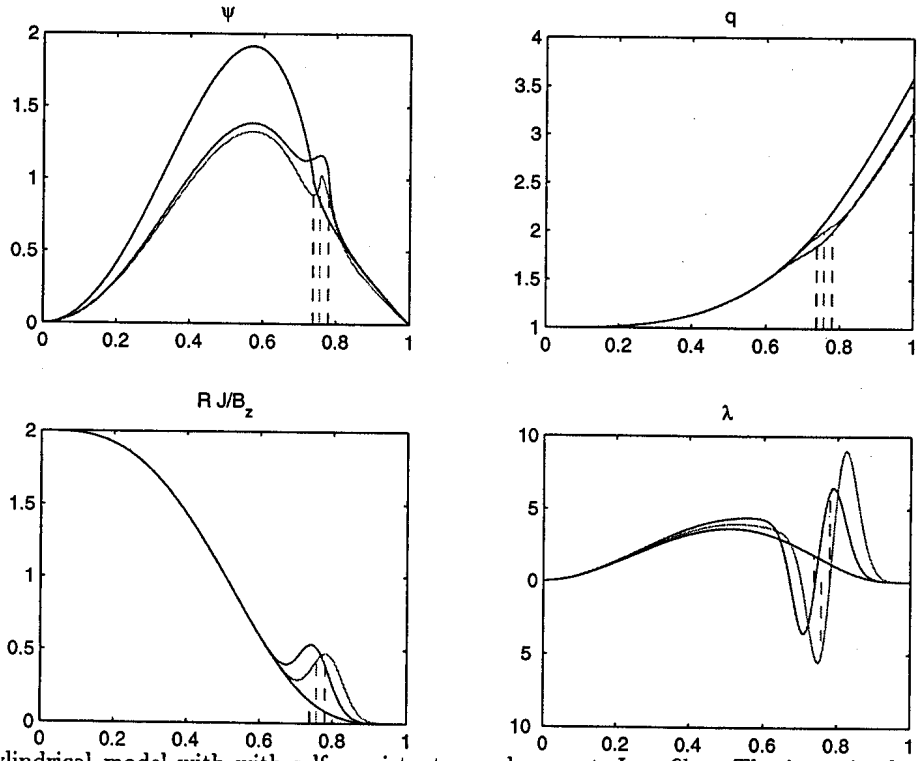

FIG. 2. Cylindrical model with with self-consistent q and current J profiles. The jump in the radial derivative takes place at the rational surface position, whose position is indicated by a vertical dashed line (top left). The rational surface moves outward (top right) due to the Gaussian current drive (bottom left). Regions of favourable current gradients are produced on either side of the rational surface (bottom right). Black curves correspond to the unperturbed equilibrium.

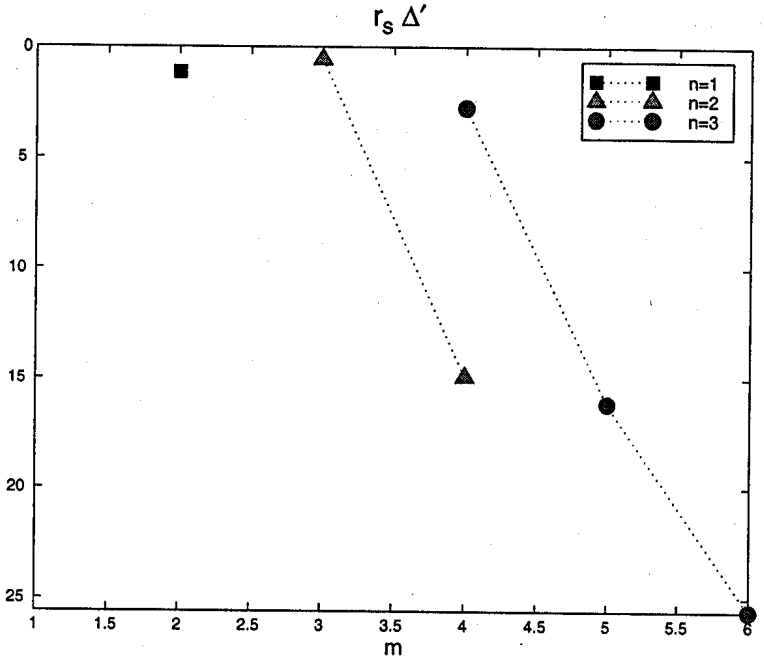

FIG. 3. The matching index Δ' is weakly stable for the 2/1, 3/2 and 4/3 modes.

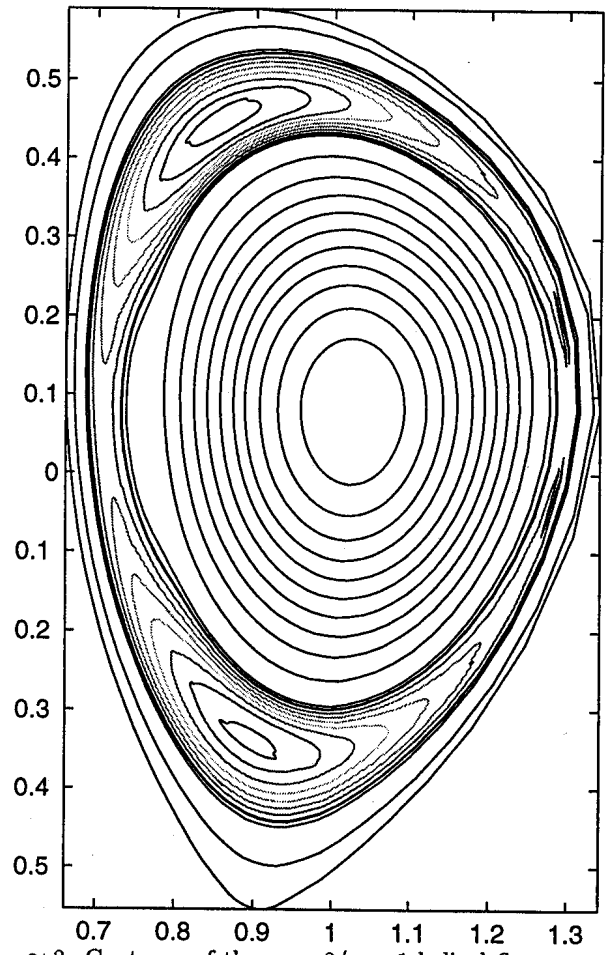

FIG. 4. ITER equilibrium with $\beta_N \approx 2$. Contours of the $m = 2/n = 1$ helical flux computed using the PEST-3 code. The island sits at $q = 2$ and $r_s\Delta' = -2.6$ in this case.

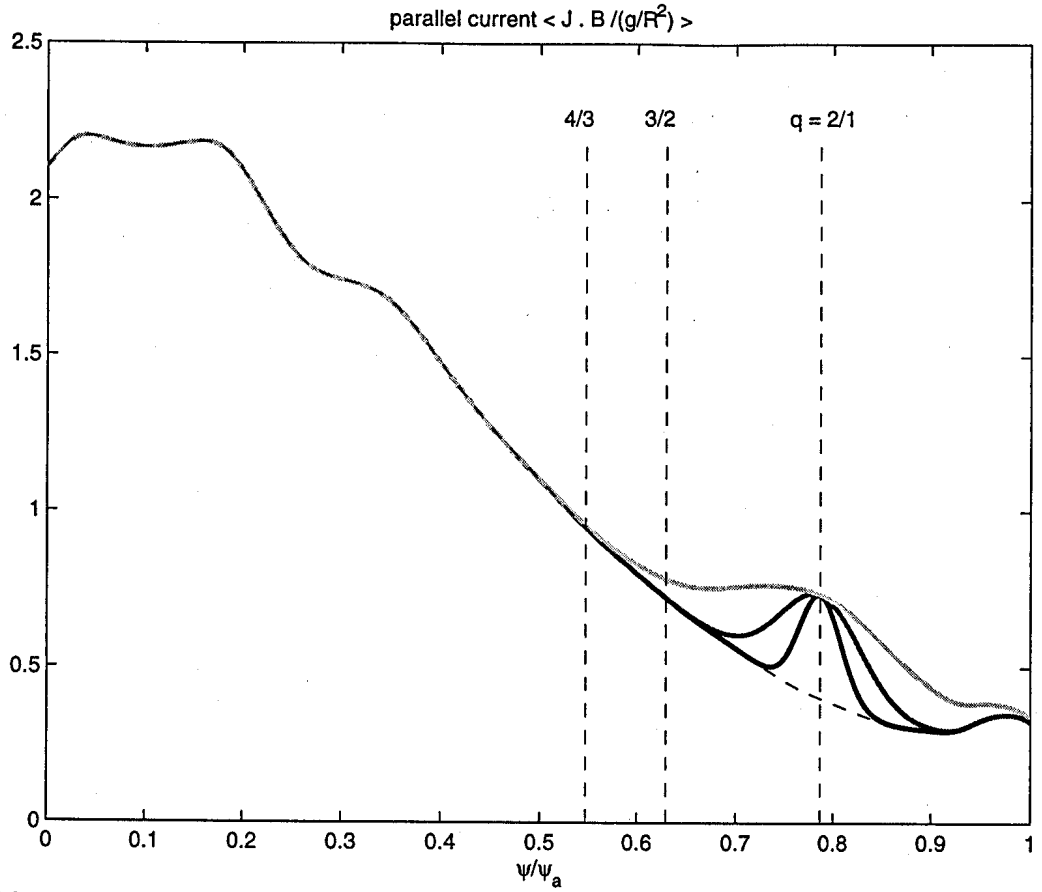

FIG. 5. Parallel current with peaked (black), medium (dark grey) and broad (light grey) CCD channel about the the $q = 2/1$ rational surface. The position of the neighbouring $q = 3/2$ and $q = 4/3$ surfaces are indicated by the vertical dashed lines.

IV. RESULTS

A. Large aspect ratio plasma

One effect not taken into account is the flattening of the safety factor profile due to the Gaussian current perturbation. A more realistic model would consist of a perturbed current density and a safety factor profile that are computed self-consistently. The result of such a model is shown in Fig. 2. The black curve is the response to the unperturbed equilibrium current density. The stabilizing effect of the incremental Gaussian current is clearly noticeable from the jump in derivatives at the rational surface. Here we observe that the stabilization is more effective when applying the Gaussian current somewhat outward of the unperturbed rational surface position, a direct consequence of the the rational surface moving toward the edge as J_{CD} increases. Note that the current drive effectively adds an odd contribution to λ, which is negative inside and positive outside the rational surface.

B. ITER equilibrium

The code PEST-3 has been used to determine Δ' for an ITER profile, as predicted immediately after a sawtooth crash. Figure 3 shows the Δ' matching data for various m/n resonant modes, $m = 2, 3, 4, 5, 6$ and $n = 1, 2, 3$. Higher m modes tend to be stable because $r_s\Delta' \to -2m$ as indicated by (16). Another factor of stabilization is the proximity of the rational surface to the conducting wall. Thus, it is found numerically that the most

dangerous modes are resonant at the 2/1, 3/2 and 4/3 surfaces. In the present case these three modes have a slightly negative Δ'.

Figure 4 is representative of the effect of a strong bootstrap current drive combined with a moderate $r_s\Delta' = -2.6$. It shows the equilibrium helical flux

$$\psi_0 = \frac{1}{(2\pi)^2}\int d\tau \mathbf{B}_0\cdot\nabla\hat{\theta},$$

to which a helical perturbation $A\cos m\hat{\theta}$ has been added [c.f. (1)]. The radial behaviour of A is computed by solving the linearized outer region stability equation but with full toroidal effects. The arbitrary constant in A is determined from the island width definition (3), after determining the fixed point of the island equation [c.f. (12)]

$$1.64\frac{\tau_R}{r_s}\frac{d}{dt}\left(\frac{w}{r_s}\right) = r_s\Delta(w) + 2.3\sqrt{\epsilon_s}\beta_p\frac{L_q}{L_p}\left(\frac{r_s}{w}\right). \tag{23}$$

Equation (23) includes the lowest order quasi-linear corrections as well as the Glasser, Greene and Johnson stabilization,

$$r_s\Delta(w) = r_s\Delta' + 3.1D_R\left(\frac{r_s}{w}\right) + 1.64\lambda_s^2\left(\frac{w}{r_s}\right)\ln\left|\frac{w}{r_s}\right|. \tag{24}$$

Higher order quasi-linear corrections and the polarization current have been on the other hand neglected.

C. Continuous Current Drive at the 2/1 surface in ITER

We have added a Gaussian CCD to the equilibrium current of the form given by (18) and solved the Grad-Shafranov equation with this modified profile. The code PEST-3 has then been run to determine Δ'. Due to the variational formulation used to solve the toroidal outer region equation, PEST-3 tends to systematically underestimate Δ'. This has been corrected by performing a careful convergence study in the number of radial mesh nodes and extrapolating to get Δ' for an "infinite" resolution.

In the absence of CCD a converged value of $r_s\Delta' = -1.14$ was found. The total parallel current is shown in Fig. 5. The curves correspond to $\sigma = 0.03$ (peaked Gaussian), $\sigma = 0.06$ (medium) and $\sigma = 0.12$ (broad). The CCD is applied inside at $\alpha = -0.5$, at the unperturbed rational surface position $\alpha = 0$ and outside at $\alpha = 0.5$. In addition, the current density J_{CD} is varied from zero to $\sim 30\%$ of the current density on axis. The total current $I_{CD} \sim J_{CD}\times\sigma$ of the Gaussian CCD amounts to $< 8\%$ of the toroidal current for the peaked Gaussian, and 30 % of the plasma current for the broad Gaussian.

The numerical results confirm our earlier predictions that the stabilization is proportional to J_{CD} and inversely proportional to the channel half-width σ, that is $\propto I_{CD}/\sigma^2$. Note the large negative values of Δ', which efficiently suppress the island. Without CCD we have $\beta_p \approx 0.41$ and $L_q/L_p \approx 1.4$ which yields an island of half-width $w/r_s \approx 0.23$. For the peaked CCD profile, a reduction of the matching index from -1.14 ($I_{CD} = 0$) to $r_s\Delta' = -5.88$ at $I_{CD}/I_0 = 0.24\%$ has been found for $\alpha = 0$.

The effectiveness of the stabilization of the CCD, however, can be lost when the favourable current gradient regions move completely to either side of the rational surface. This is more likely to happen at moderate to large I_{CD} and when applying the CCD inward (triangles pointing to the left), as a result of the flattening of the q profile. The model developed in § III still applies provided α reflects the distance of the CCD from the *new* rational surface position. We know from the model of § III that in the worst scenario, this destabilization can reach 30 % $\approx [h(\alpha)_{max} - 1]/[1 - h(\alpha)_{min}]$ of the maximum attainable stabilization in Δ' at $\alpha = 0$. Comparing left pointing triangles with both diamonds and right-triangles for every current, we find that this destabilization nowhere exceeds 30 %. For the reasons mentioned above the most robust stabilization is obtained for $\alpha \sim 0.5$.

Small current amplitudes have already a large impact on the reduction of the saturation width to below 5% of the minor radius, as shown in Fig. 6. The reduction in w/r_s is approximately proportional to $(-\Delta')^{-1}$. However, at larger current magnitudes, the flattening of the current profiles removes some stabilization due to the quasi-linear terms in (23). In general, the relation between the saturation width and Δ' is monotonic, although there are

cases where the quasi-linear stabilization term plays the dominant role when λ_s becomes large.

The effect of a CCD at the 2/1 surface is also investigated on neighbouring rational surfaces. With the exception of the cases where the CCD overlaps these rational surfaces, the CCD is slightly destabilizing as expected. For any parameter choice, however, the 5/2 surface remains stable (data not shown), whereas there is a large parameter range for the 3/2 surface where this destabilization remains modest. The choice of $\alpha \approx 0.5$ combined with $\sigma \approx 0.05$ and $I_{CD}/I_0 \approx 0.02 - 0.05$, for instance, reduces Δ' at the 2/1 surface to -20 while barely affecting the stability at the 3/2 surface.

D. Continuous Current Drive at the 3/2 surface

In the absence of additional CCD, the 3/2 surface is characterized by $r_s\Delta' = -0.5$, $\beta_p \approx 0.57$ and $L_q/L_p \approx 1.4$. In spite of such weak Δ' and and yet strong bootstrap current drive, the saturation half-width is smaller than for the 2/1 mode. This is due to the quasi-linear stabilization, with λ_s^2 at 3/2 being 3.6 times larger than at 2/1. Accordingly, a large decrease in Δ' does not entirely translate into reduced w, as can be observed in Fig. 8.

The stabilization of Δ' for the 3/2 mode with CCD at the 3/2 surface is similar to the previous case. This is not surprising as the reduction in Δ' due to the CCD dominates over other equilibrium features, thereby justifying the assumptions made in § III.

To avoid destabilizing the 2/1 surface, it appears more advantageous to use smaller CCD amplitudes well centered at the 3/2 surface. For instance $I_{CD}/I_0 \approx 0.02$ combined with $\alpha \approx 0$ allows one to reduce the half width to below 5% without further destabilizing the 4/3 and 2/1 surfaces.

V. SUMMARY

We have shown that the most unstable modes for a test ITER equilibrium are likely to have 3/2, 2/1 and 4/3 helicities. In addition there can be 1/1 and 2/2 sawtooth crashes, which through toroidal and nonlinear coupling can trigger the growth of islands at the 4/3 and 3/2 rational surfaces.

The saturation of these tearing modes relies on a negative matching index Δ' and/or quasi-linear effects which originate in the profile readjustment as the island develops. The pressure profile corrections are taken care by the Glasser, Greene and Johnson term in the island evolution equation. Alternatively, the pressure flettening can be absorbed into the Δ' index as in the work of Bishop *et al.* [31], who also found a stabilization that is inversely proportional to the island width. The dependence of this stabilization competes with the bootstrap current drive. However, it is found in particular for the studied ITER equilibrium that the Glasser, Greene and Johnson stabilization is negligeable compared to the bootstrap current drive.

Next we find by means of a heuristic derivation that the quasi-linear term due to the flattening of the current profile amounts to a $w \log w$ term, as predicted by Thyagaraja. Such a term is stronger than the one proportional to w adopted by other authors. We believe that this quasi-linear term plays an important role. In particular, the 3/2 mode in ITER has a smaller saturation width than the 2/1 mode despite a more positive Δ' and a stronger bootstrap current drive.

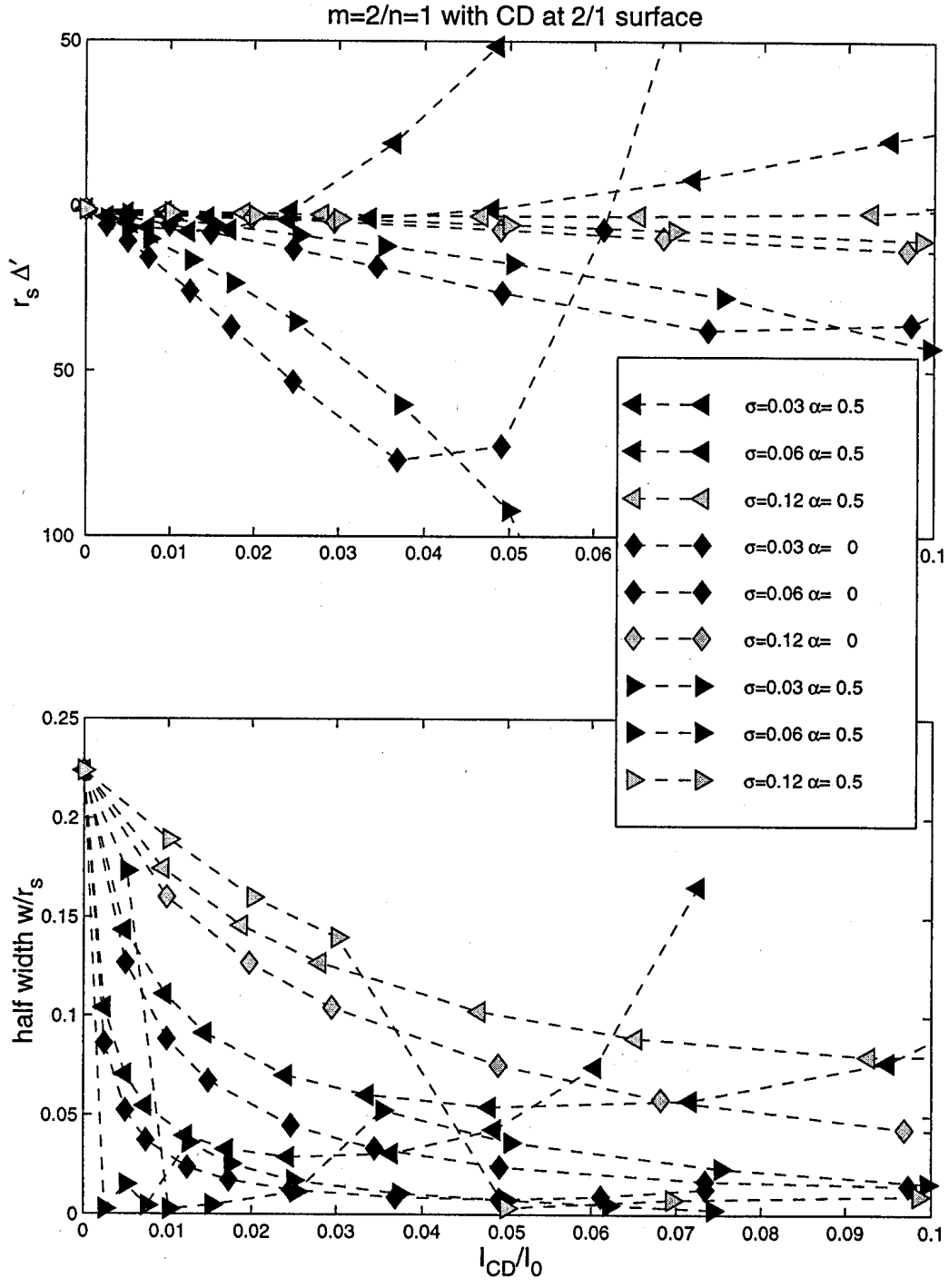

FIG. 6. Matching index (top) and half-island width vs the CCD normalized to the plasma current. Triangles pointing to the left correspond to a CCD shifted inward by $\alpha = -0.5$, diamonds to a CCD centered at the original rational surface 2/1 position, and triangles pointing to the right to a CCD shifted outward by $\alpha = 0.5$.

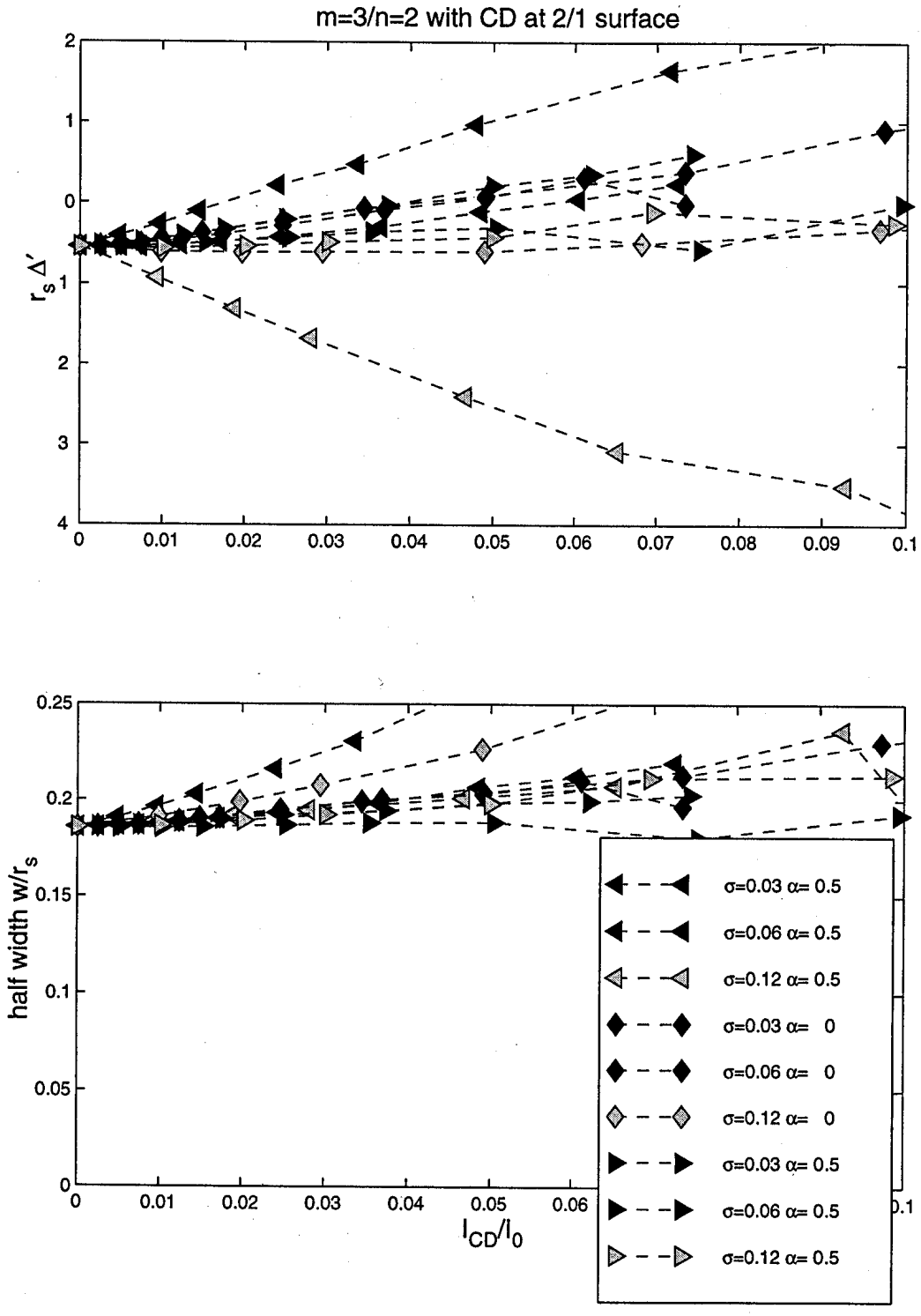

FIG. 7. Current drive located at $q = 2/1$ surface has a small destabilizing influence at the 3/2 surface.

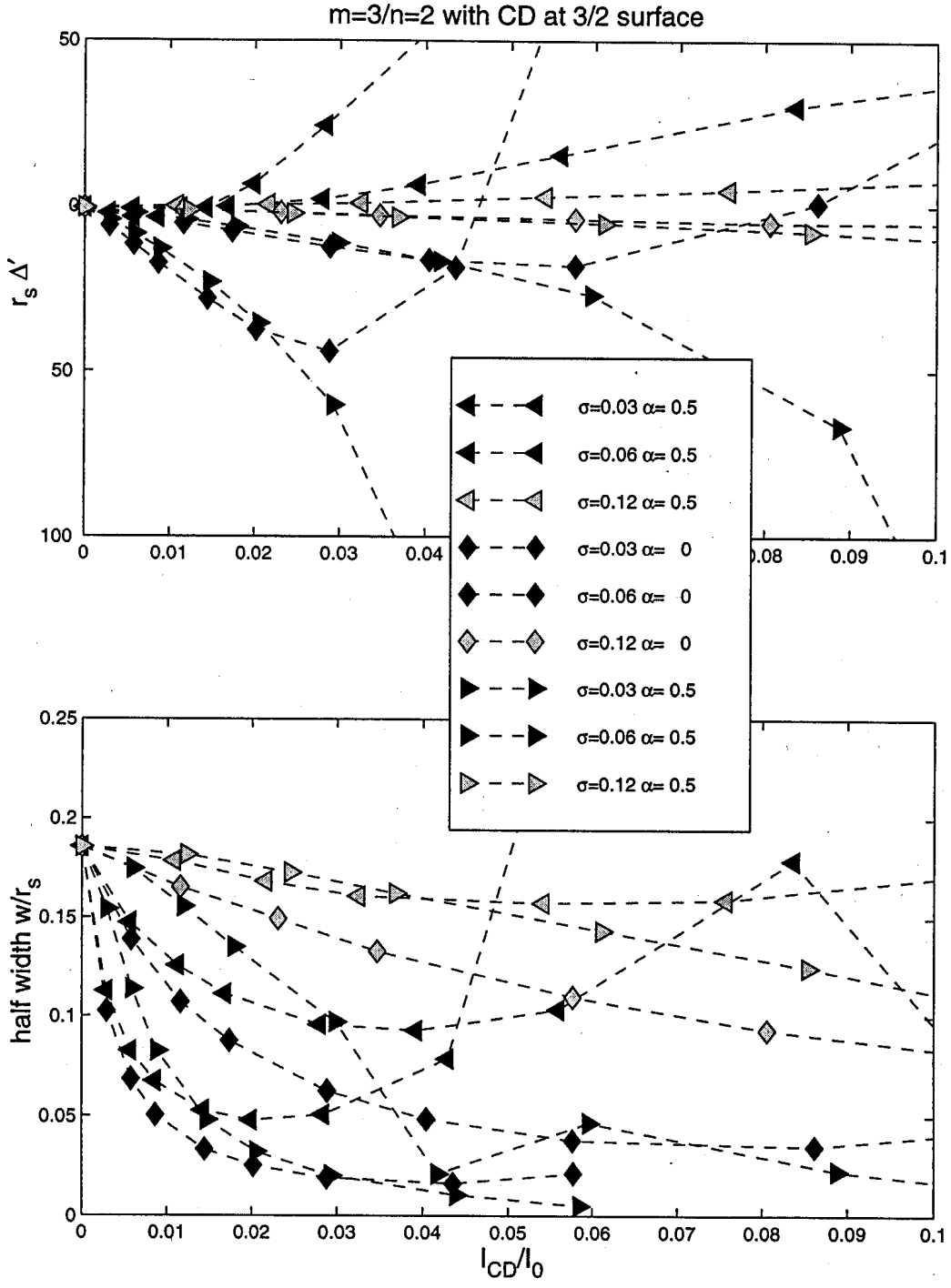

FIG. 8. Stabilization of the 3/2 mode after applying a localized current drive in the vicinity of the $q = 3/2$ surface.

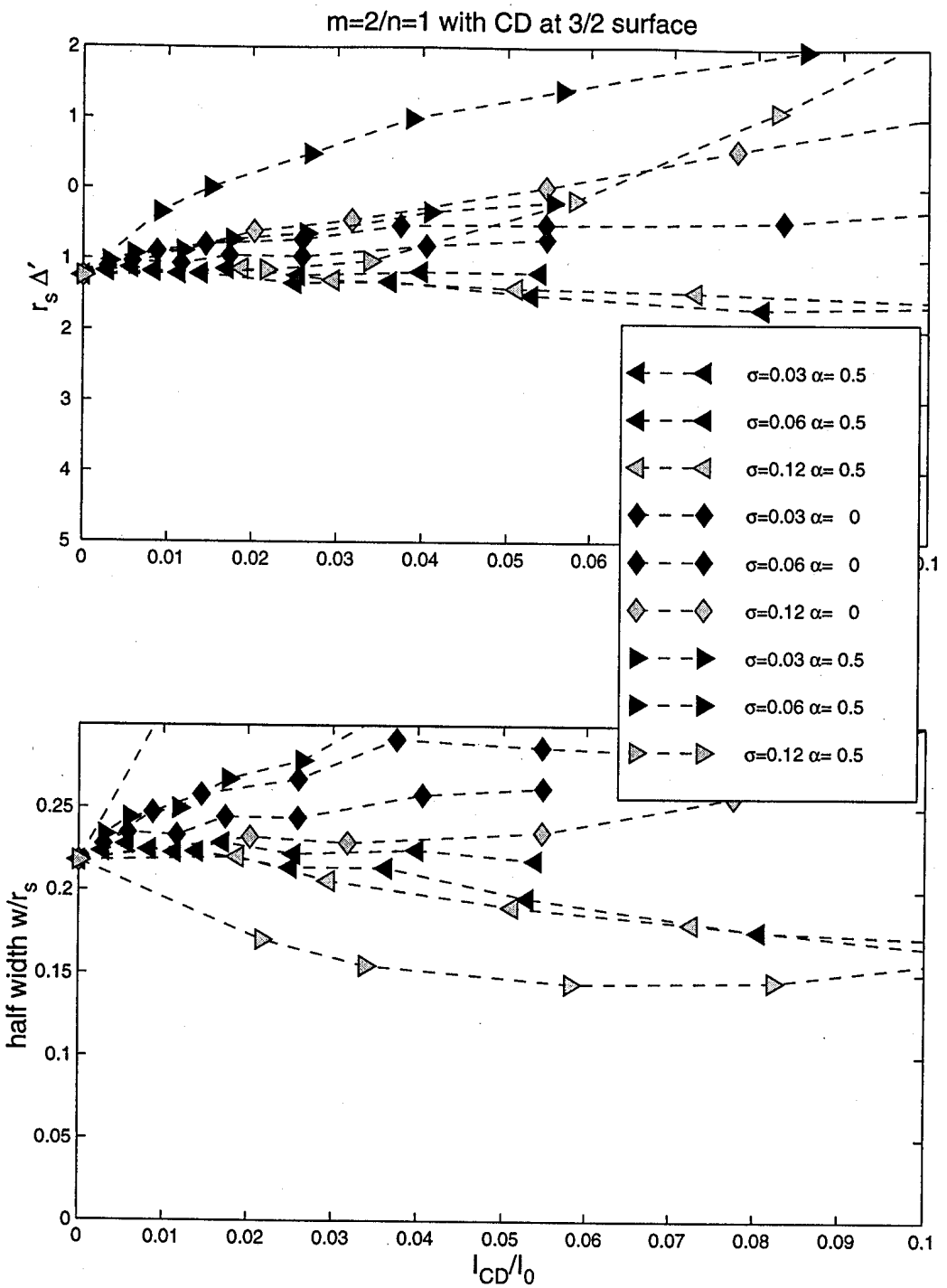

FIG. 9. Current drive located at $q = 3/2$ surface has a small destabilizing influence at the 2/1 surface.

In spite of these stabilizing contributions, our ITER test equilibrium reveals that the plasma would presumably disrupt in the absence of additional stabilization. To remedy this, we have proposed a scheme whereby a localized, continuous Gaussian current is applied about the rational surface with the aim of creating regions of favourable current gradients on either side. This is a purely ideal MHD effect which translates into a more negative Δ', the reduction being proportional to the current drive density at the Gaussian peak and inversely proportional to the current channel width (or proportional to the total current contained in the Gaussian bump over the square of the channel width). A similar study was previously

undertaken by Westerhof [29]. However, in contrast to his results, both our analytic model and the numerical simulations in toroidal geometry show that the stabilizing effect can be made arbitrarily large, at least up to the point where the assumptions of the asymptotic matching model break down. Another practical limitation comes from the difficulty in predicting the rational surface position in presence of the current drive beforehand, due to the resulting modification of the safety factor profile. This problem is exacerbated by the destabilizing effect of the current drive away from the rational surface. A small deviation from the exact position can be tolerated; in (22) we provide a simple rule to estimate the precision at which the rational surface must be aimed at. It appears more suitable to aim just outside the rational surface as the current drive introduces a flattening of the q profile which moves the rational surface outward. This is certainly true for the 2/1 mode which has in its outside vicinity only very stable modes. For the 3/2 mode we suggest a smaller current drive amplitude combined with a narrow current channel to avoid the destabilization of the 2/1 and 4/3 modes. The present study also indicates that stabilization of both the 3/2 and 2/1 modes may be required for ITER.

In determining the island sizes we have relied on the asymptotic matching approximation, which is rigorously valid only in the limit where the island width goes to zero. It is important to recall that this approach also assumes that equilibrium quantities (including current drive) vary on a much larger length scale than the island width. Thus, the channel current width must $\gg$ the island width. This condition was not always satisfied in the present study.

The opposite limit, namely when the current drive channel is smaller than the island width, has been treated by Hegna and Callen [14]. These authors find a stabilizing contribution $D_{aux}\eta_{aux}(r_s/2w)^2$, where $D_{aux} \approx 16 I_{CD} R q_s/(\pi \hat{s} B r_s^2)$ is proportional to the driven current I_{CD} and η a function decreasing monotonically with the broadening of the current distribution inside the island separatrix. High efficiency is achieved when the current is a δ function at the island O-point ($\eta = 1$), while reaching a minimum value of $\eta \approx 0.4$ when the current is uniformely distributed within the separatrix. Comparing our model to the one of Hegna and Callen when $\sigma = w$, we find a stabilization of comparable magnitude. Thus, the correction to Δ' as given by (20) connects smoothly to the expression of Hegna and Callen as the current channel width decreases. Not surprisingly, the finite width island width regularizes (20) in the limit of $\sigma \to 0$ by preventing Δ' to become infinite.

Note finally that applying a current drive inside the island requires the current drive to be modulated to account for the island rotation. The stabilization using a continuous current drive as opposed to a pulsed one has the merit of simplicity while giving the same dependence in current and channel width.

ACKNOWLEDGMENTS

This work was partly supported by the Swiss National Fund and Euratom.

We are grateful to M. N. Rosenbluth for stimulating this work and for providing an analytic solution to (19).

---

[1] W. X. Qu and J. D. Callen, Report UWPR-85-5, University of Wisconsin (unpublished).
[2] R. Carrera, R. D. Hazeltine, and M. Kotschenreuther, Phys. Fluids **29**, 899 (1986).
[3] H. P. Furth, P. H. Rutherford, and H. Selberg, Phys. Fluids **16**, 1054 (1973).
[4] A. Pletzer, Phys. Plasmas **4**, 3141 (1997).
[5] H. P. Furth, J. Killeen, and M. N. Rosenbluth, Phys. Fluids **6**, 459 (1963).
[6] R. Fitzpatrick, Phys. Plasmas **2**, 825 (1995).
[7] H. R. Wilson, J. W. Connor, R. J. Hastie, and C. C. Hegna, Phys. Plasmas **3**, 248 (1996).
[8] R. J. LaHaye, accepted for publication in Nucl. Fusion (1998).
[9] F. Porcelli, D. Boucher, and M. N. Rosenbluth, Plasma Phys. Contr. Fusion **38**, 2163 (1996).
[10] A. Thyagaraja, Phys. Fluids **24**, 1716 (1981).
[11] R. B. White and D. A. Monticello, Phys. Fluids **20**, 800 (1977).
[12] C. C. Hegna and J. D. Callen, Phys. Plasmas **1**, 2308 (1994).

[13] F. Perkins, R. W. Harvey, M. Makovski, and M. N. Rosenbluth, Technical Report No. APS Poster (unpublished).
[14] C. C. Hegna and J. D. Callen, Phys. Plasmas **4**, 2940 (1997).
[15] H. Zohm, Phys. Plasmas **4**, 3433 (1997).
[16] P. H. Rutherford, Phys. Fluids **16**, 1903 (1973).
[17] W. A. Newcomb, Ann. Phys. **10**, 232 (1960).
[18] M. Bineau, Nucl. Fusion **2**, 130 (1962).
[19] M. Kotschenreuther, R. D. Hazeltine, and P. J. Morrison, Phys. Fluids **28**, 294 (1985).
[20] C. C. Hegna and J. D. Callen, Phys. Plasmas **1**, 3135 (1994).
[21] M. Zabiégo and X. Garbet, Phys. Plasmas **2**, 1236 (1995).
[22] Z. Chang *et al.*, Phys. Rev. Lett. **74**, 4663 (1995).
[23] L. E. Zakharov, A. I. Smolyakov, and A. A. Subbotin, Sov. J. Plasma Phys. **16**, 451 (1991).
[24] R. L. Dewar and A. Pletzer, J. Plasma Phys. **43**, 291 (1990).
[25] A. Pletzer and R. L. Dewar, J. Plasma Phys. **45**, 427 (1991).
[26] A. H. Glasser, J. M. Greene, and J. L. Johnson, Phys. Fluids **18**, 875 (1975).
[27] A. D. Miller and R. L. Dewar, J. Comput. Phys. **66**, 356 (1986).
[28] A. Pletzer, A. Bondeson, and R. L. Dewar, J. Comput. Phys. **115**, 530 (1994).
[29] E. Westerhof, Nucl. Fusion **27**, 1929 (1987).
[30] H. R. Strauss, Phys. Fluids **24**, 2004 (1981).
[31] C. M. Bishop, J. W. Connor, R. J. Hastie, and S. C. Cowley, Plasma Phys. and Controlled Fusion **33**, 389 (1991).